Journal of Physics: Conference Series

Measurement of electroweak boson production in *pp*, *p*+Pb and Pb+Pb collisions with the ATLAS detector

To cite this article: Piotr Janus and on behalf of theATLAS Collaboration 2019 *J. Phys.: Conf. Ser.* **1390** 012023

Journal of Physics: Conference Series **1390** (2019) 012023 doi:10.1088/1742-6596/1390/1/012023

Measurement of electroweak boson production in pp, p+Pb and Pb+Pb collisions with the ATLAS detector

Piotr Janus, on behalf of the ATLAS Collaboration[1]

AGH University of Science and Technology
Faculty of Physics and Applied Computer Science
Al. Mickiewicza 30, 30-059 Cracow, Poland

E-mail: piotr.janus@cern.ch

Abstract. Measurement of electroweak boson production in different collision systems are of great interest to understanding the partonic structure of heavy nuclei, and serve as a constraint on the initial state in larger collision systems. Their production yields in Pb+Pb with respect to pp collisions provide direct tests of both binary collision scaling and possible modification of parton distribution functions (nPDF) due to nuclear effects. Further, the p+Pb collisions provide a relatively clean environment to study nPDFs in detail. The ATLAS detector has a broad acceptance with excellent performance even in the high occupancy environment of central heavy-ion collisions. In this proceedings the latest ATLAS results on W and Z boson production at the centre-of-mass energy of 5.02 TeV are presented, including updated precise result production in pp collisions. Also photon yields are reported in 8.16 TeV in different collision systems are presented.

1. Introduction

The Relativistic Heavy Ion Colider (RHIC) showed that strongly interacting matter produced in collision of two heavy nuclei takes the form of quark gluon plasma (QGP) [1]. In such medium produced colour particles are expected to lose energy which leads to a phenomenon known as jet quenching. Suppression of charged hadron yields in heavy-ion (HI) collisions was already reported by experiments at RHIC and the LHC [2–4]. A direct way to study the initial stage of proton-proton (pp), proton-nucleus and nucleus-nucleus collisions is to measure production of colourless electroweak (EW) bosons, namely high-energy photons, $W^{\pm}$ and Z. These bosons are created at the very early stage of the collision in the hard parton-parton interaction. Products of leptonic decays of $W^{\pm}$ and Z are expected to not interact substantially with the QGP, making them useful probes of the QGP. This unique feature makes them sensitive to the initial geometry of the HI collision and nuclear modifications to parton distribution functions (nPDF). A measurement of direct photon production [5] by the PHENIX experiment at RHIC showed that photon rates scale with the nuclear thickness function. Very similar conclusions came from the first measurements of electroweak vector bosons in Pb+Pb collisions performed by the ATLAS and CMS experiments [6–10]. In principle their production rates were found to be independent of the presence of QGP. Furthermore, the weak boson production in p+Pb and Pb+Pb collisions may differ from the pp system. There are two main sources of these differences.

The first one is related to the presence of neutrons in the nucleus which have different quark composition compared to protons. Secondly, EW bosons production can be affected by effects arising from partons being bound in the nucleus where the PDF of the free nucleon might be modified leading to parton depletion or enhancement [11].

This proceedings covers the most recent measurements on $W^{\pm}$ and Z production in the pp and Pb+Pb system at $\sqrt{s_{\rm NN}} = 5.02$ TeV and prompt photon production in the p+Pb system at $\sqrt{s_{\rm NN}} = 8.16$ TeV. They are based on data collected in 2015 and 2016 by the ATLAS experiment [12] at the LHC.

2. W and Z production in pp collisions

Measurements of $W^{\pm}$ and Z boson production in pp collisions provide a benchmark for the understanding of quantum chromodynamics (QCD) and EW processes. They also serve as an important reference for weak-boson production in heavy-ion collisions. The ATLAS experiment has measured $W^{\pm}$ and Z boson production in pp collisions at centre-of-mass energy of $\sqrt{s} = 5.02$ TeV [13] using data corresponding to an integrated luminosity of 25.0 pb^{-1}. This dataset is characterised by a relatively low pile-up contribution with mean number of pp interactions per bunch crossing equal to 1.5. Samples of Monte Carlo (MC) simulated events are used to evaluate the selection efficiency for signal events and the contribution of several background processes. All of the samples are processed with the Geant4-based simulation [14, 15] of the ATLAS detector. Dedicated efficiency and calibration studies with data are used to derive correction factors to account for residual differences between experiment and simulation. Measurement includes differential cross sections convoluted with leptonic branching ratios for the processes $W^+ \to \ell^+\nu$, $W^- \to \ell^-\nu$ and $Z \to \ell^+\ell^-$ ($\ell = e, \mu$), respectively. Electron and muon decay channels are analysed and combined together. The fiducial phase space is defined by detector acceptance and lepton kinematics:

- for W production: $p_{\rm T}^{\ell} > 25$ GeV, $p_{\rm T}^{\nu} > 25$ GeV, $|\eta_\ell| < 2.5$, $m_{\rm T} > 40$ GeV
- for Z production: $p_{\rm T}^{\ell} > 20$ GeV, $|\eta_\ell| < 2.5$, $66 < m_{\ell\ell} < 116$ GeV.

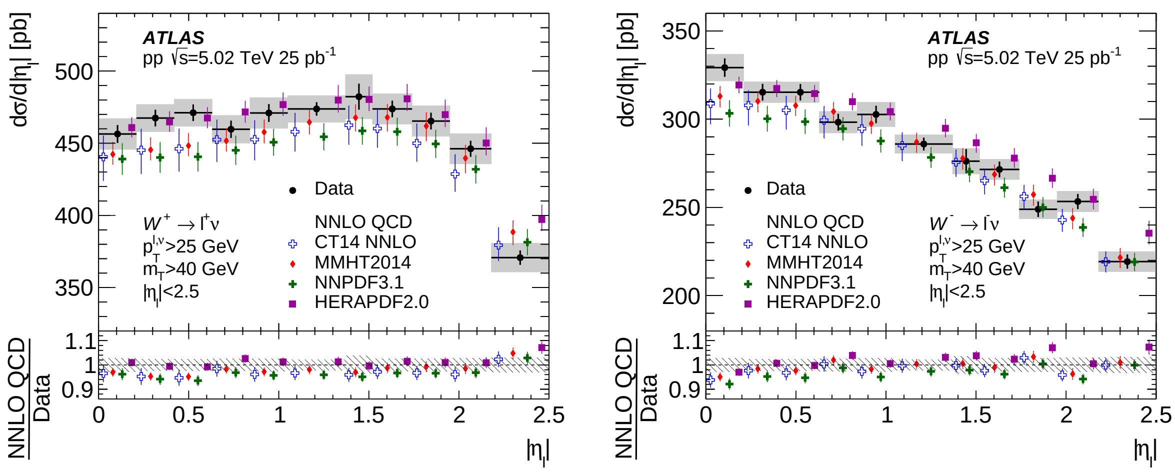

Figure 1. Differential cross sections for W^+ (left) and W^- (right) boson production as a function of absolute decay lepton pseudorapidity compared with theoretical predictions. Statistical and systematic uncertainties are shown as error bars and shaded rectangles, respectively. The lower panels show the ratios of predictions to the measured differential cross sections [13].

Journal of Physics: Conference Series **1390** (2019) 012023 doi:10.1088/1742-6596/1390/1/012023

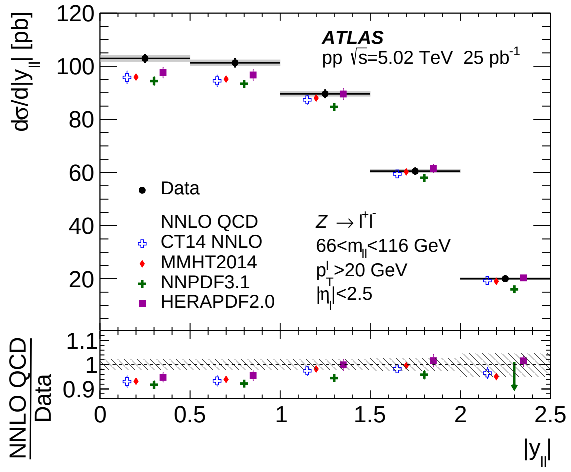

Figure 2. Differential cross section for Z boson production as a function of absolute lepton-pair rapidity compared with theoretical predictions. Statistical and systematic uncertainties are shown as error bars and shaded rectangles, respectively. The lower panels show the ratios of predictions to the measured differential cross sections [13].

The measured cross sections are compared with theoretical predictions obtained using a modified version of DYNNLO 1.5 [16, 17] optimised for speed of computation. Differential cross sections for W and Z boson production are shown in Figures 1 and 2 as a function of $|\eta_\ell|$ and the lepton-pair rapidity $|y_{\ell\ell}|$, respectively. The cross sections for the combined measurements are compared to theoretical predictions obtained with the CT14 [18], NNPDF3.1 [19], MMHT14 [20] and HERAPDF2.0 [21] PDF sets. In some regions of phase space, a comparison of the differential cross sections shows systematic deviations of the predictions obtained with recent PDF sets from the measured values. These deviations are largest for W^+ boson production and at central rapidity for Z boson production.

3. W and Z production in Pb+Pb collisions

The W and Z boson production has been measured in Pb+Pb collisions at $\sqrt{s_{\rm NN}} = 5.02$ TeV using data corresponding to an integrated luminosity of 0.49 nb^{-1} [22, 23]. Samples of MC simulated events are used with similar manner to the measurement described in the Section 2 to evaluate the selection efficiency for signal events and the contribution of several background processes. Also, dedicated efficiency studies are used to derive correction factors to account for residual differences between experiment and simulation. Differential yields for processes $W^+ \to \mu^+\nu$, $W^- \to \mu^-\nu$ and $Z \to \mu^+\mu^-$ are measured. The fiducial phase space is defined by detector acceptance and muon kinematics:

- for W production: $p_{\rm T}^{\mu} > 25$ GeV, $p_{\rm T}^{\nu} > 25$ GeV, $0.1 < |\eta_\mu| < 2.4$, $m_{\rm T} > 40$ GeV
- for Z production: $p_{\rm T}^{\mu} > 20$ GeV, $|\eta_\mu| < 2.5$, $66 < m_{\mu\mu} < 116$ GeV.

Figure 3 presents Z boson yields per minimum-bias (MB) event scaled by the average nuclear thickness function $\langle T_{\rm AA}\rangle$ as a function of $|y^Z|$ for three selected centrality intervals compared to the measurement in the pp system. Good agreement with the model predictions and measured pp data points is observed. Only slight excess is observed in the most peripheral class of events. The nuclear modification factor is also shown in the lower panel. No significant deviations from unity indicates small impact of nuclear effects.

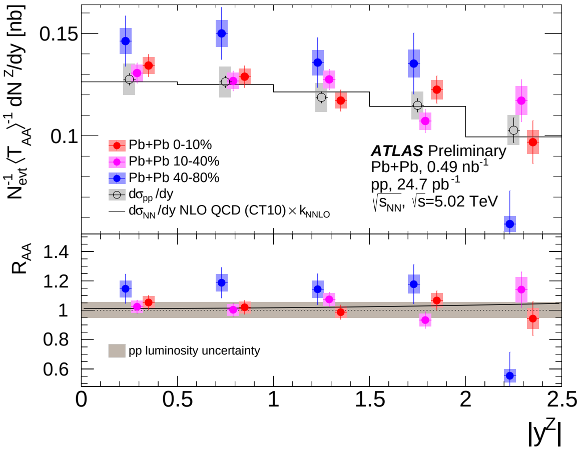

Figure 3. Upper panel presents Z-boson yields per MB event in three centrality intervals divided by $\langle T_{\mathrm{AA}} \rangle$ (filled circles) and differential cross section measured in pp (open circles) as a function of $|y^Z|$. Ratios of Pb+Pb results to *pp* result in three centrality intervals are shown in the bottom panel. The pp luminosity uncertainty (5.4%) is indicated as a band around unity. The statistical and systematic uncertainties are presented by bars and shaded boxes, respectively. Results of the Powheg-based model using CT10 PDF are also shown as a histogram [23].

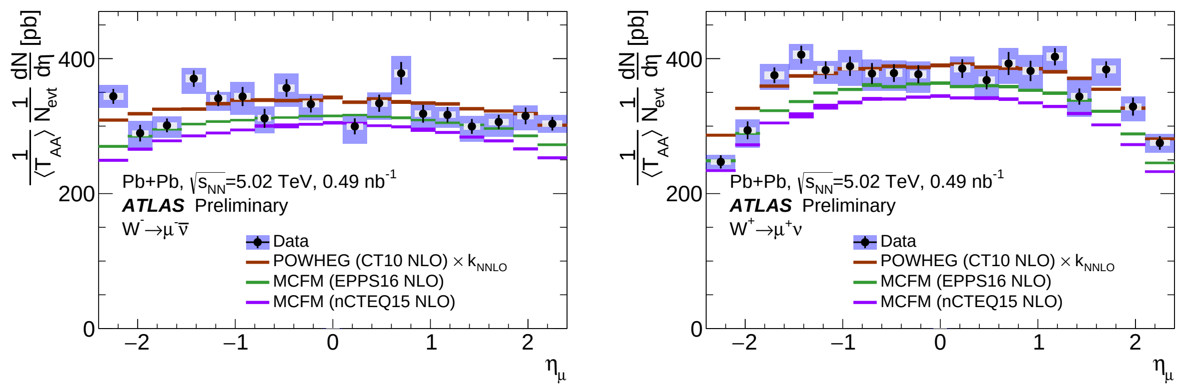

Figure 4. Differential production yields per MB event divided by $\langle T_{\mathrm{AA}} \rangle$ for $W^+ \rightarrow \mu^+\nu$ (left) and $W^- \rightarrow \mu^-\nu$ (right). Error bars represent statistical uncertainties. Systematic and statistical uncertainties added in quadrature are shown as the filled boxes, while the systematic uncertainties related to $\langle T_{\mathrm{AA}} \rangle$ are presented by the empty boxes. The width of the theory bands reflects MC statistical uncertainties [22].

Figure 4 shows the differential production yields per MB event divided by $\langle T_{\mathrm{AA}} \rangle$ as a function of η_μ separately for W^+ and W^- bosons extracted from the $0-80\%$ centrality range. The data are compared to Powheg predictions scaled by the k_{NNLO}[2] factor using CT10 free-nucleon PDF. The MC expectations are consistent with the data. Two predictions based on MCFM, using the most recent nuclear modifications to PDF, EPPS16 [24] and nCTEQ15 [25], are also shown.

[2] The scaling factor, k_{NNLO}, scales W boson production cross sections to NNLO accuracy using DYNNLO calculations with the CT14nnlo PDF set.

They both underestimate the data, however a 2-3% difference between the NNLO-scaled Powheg and MCFM predictions is expected due to the different order of the QCD calculations, i.e. the contribution of the NNLO radiative effects.

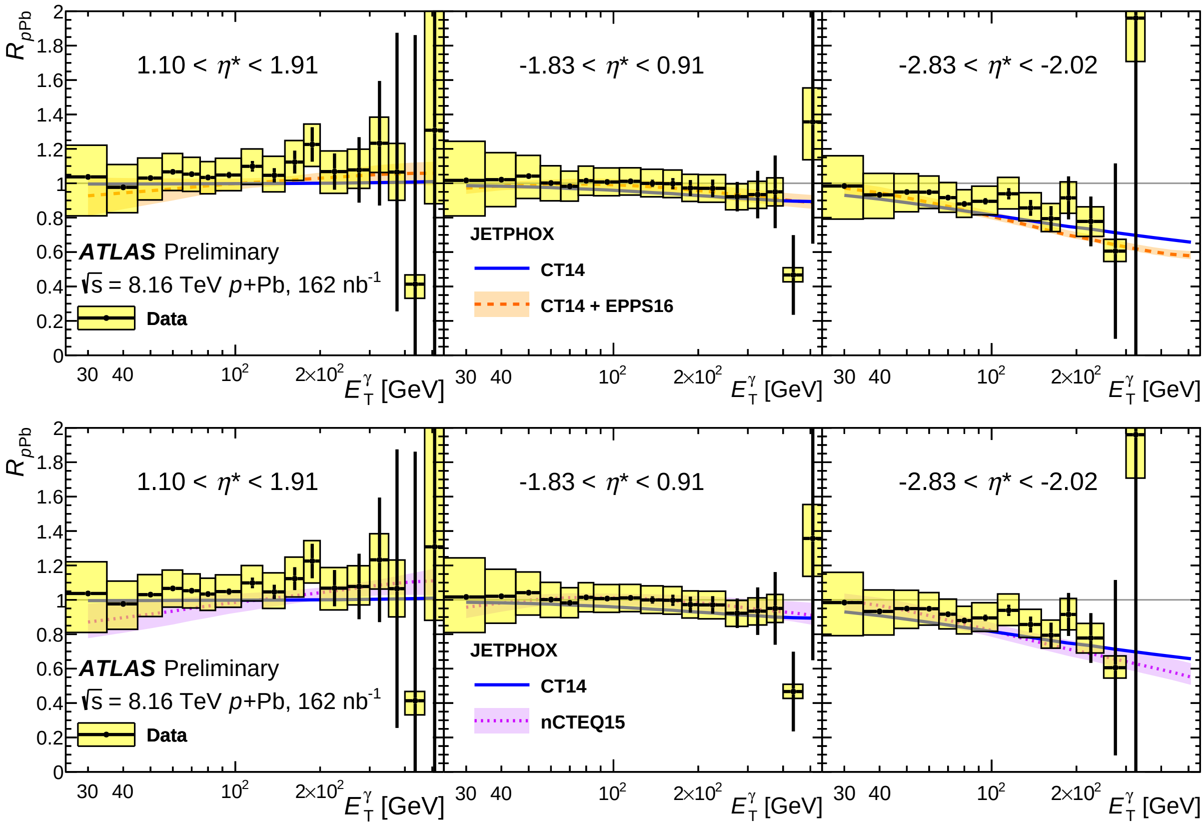

Figure 5. Nuclear modification factor R_{pPb} for isolated, prompt photons as a function of E_{T}^{γ}, shown for different η^* selections in each panel. The data are identical in each row, but show comparisons to the expectations based on Jetphox with the EPPS16 nuclear PDF set (top) or with the nCTEQ15 nuclear PDF set (bottom). In all plots, the yellow boxes and vertical bars correspond to total systematic and statistical uncertainties on the data, respectively. The orange and purple bands correspond to the systematic uncertainties on the calculations [26].

4. Prompt photon production in p+Pb collisions

Data used in prompt photon production measurement [26] were collected with the ATLAS detector during the p+Pb collision running period of 2016 and corresponds to an integrated luminosity of 162 nb^{-1}. Photon production cross-sections are reported for photons with $E_{\mathrm{T}}^{\gamma} >$ 25 GeV in three pseudorapidity intervals in the nucleon-nucleon frame: $-2.83 < \eta^* < -2.02$, $-1.83 < \eta^* < 0.91$ and $1.1 < \eta^* < 1.91$. The measurement phase space includes also isolation criterion: $E_{\mathrm{T}}^{\mathrm{iso}} < 4.8 + 4.2 \times 10^{-3} E_{\mathrm{T}}^{\gamma}$ [GeV].

The R_{pPb} is defined as the ratio of the cross-section in p+Pb collisions to the lead nuclear mass number (A) multiplied by the cross-section in pp collisions at the same $\sqrt{s}$:

$$R_{p\mathrm{Pb}} = \frac{d\sigma^{p+\mathrm{Pb}\rightarrow\gamma+X}/dE_{\mathrm{T}}^{\gamma}}{A \cdot d\sigma^{pp\rightarrow\gamma+X}/dE_{\mathrm{T}}^{\gamma}}. \quad (1)$$

Figure 5 shows the nuclear modification factor $R_{p\mathrm{Pb}}$ as functions of E_{T}^{γ} and η^{*}. The $R_{p\mathrm{Pb}}$ is consistent with unity at forward pseudorapidities and at low to moderate E_{T}^{γ} at mid-rapidity what is indicating that isospin or other nuclear effects are small. Deviations from unity of $R_{p\mathrm{Pb}}$ are visible at high E_{T}^{γ} and backward pseudorapidity. This feature primarily reflects the difference in the up and down quark composition of the nucleus relative to the proton. This effect is present in the Jetphox theory curve in blue which includes the proton-neutron asymmetry and the free proton PDF set CT14. Within the present uncertainties, the central values of the data are consistent with both the free proton PDFs and with the small effects expected from a nuclear modification of the parton densities.

5. Conclusions

Measurements of EW boson production have been reported based on pp, p+Pb and Pb+Pb data collected at $\sqrt{s_{\mathrm{NN}}} = 5.02$ TeV and $\sqrt{s_{\mathrm{NN}}} = 8.16$ TeV by the ATLAS experiment at the LHC. A comparison of the differential cross sections of W and Z boson production in pp data shows $1-2\sigma$ deviations from the predictions obtained with many of the recent PDF sets. Reported W and Z boson yields in Pb+Pb collisions are in good agreement with the model predictions. Results of W boson measurement seems to favour predictions calculated with CT10 free-nucleon PDF set. Measured nuclear modification factor $R_{p\mathrm{Pb}}$ for prompt photon production is mostly consistent with unity. Deviations from unity of $R_{p\mathrm{Pb}}$ are visible at high E_{T}^{γ} and backward pseudorapidity which are result of the isospin effect.

Acknowledgements

This work was partly supported by the National Science Centre of Poland under grant numbers DEC-2016/23/B/ST2/01409 and DEC-2018/28/T/ST2/00047, by the AGH UST grant No. 15.11.220.717/14 and by PL-GRID infrastructure.

References

[1] Adcox K *et al.* 2005 *Nucl. Phys. A* **757** 184
[2] Adler S S *et al* 2004 *Phys. Rev. C* **69** 034910
[3] ATLAS Collaboration 2015 *JHEP* **09** 050
[4] CMS Collaboration 2012 *Eur. Phys. J. C* **72** 1945
[5] Afanasiev S *et al.* 2012 *Phys. Rev. Lett.* **109** 152302
[6] ATLAS Collaboration 2016 *Phys. Rev. C* **93** 034914
[7] CMS Collaboration 2012 *Phys. Lett. B* **710** 256
[8] ATLAS Collaboration 2013 *Phys. Rev. Lett.* **110** 022301
[9] ATLAS Collaboration 2015 *Eur. Phys. J. C* **75** 23
[10] CMS Collaboration 2012 *Phys. Lett. B* **715** 66
[11] Vogt R 2001 *Phys. Rev. C* **64** 044901
[12] ATLAS Collaboration 2008 *JINST* **3** S08003
[13] ATLAS Collaboration 2018 *Preprint* 1810.08424 [hep-ex]
[14] Agostinelli S *et al.* 2003 *Nucl. Instrum. Meth. A* **506** 250
[15] ATLAS Collaboration 2010 *Eur. Phys. J. C* **70** 823
[16] Catani S and Grazzini M 2007 *Phys. Rev. Lett.* **98** 222002
[17] Catani S, Cieri L, Ferrera G, Florian D and Grazzini M 2009 *Phys. Rev. Lett.* **103** 082001
[18] Dulat S *et al.* 2016 *Phys. Rev. D* **93** 033006
[19] Ball R D *et al.* 2017 *Eur. Phys. J. C* **77** 663
[20] Harland-Lang L A, Martin A D, Motylinski P and Thorne R S 2015 *Eur. Phys. J. C* **75** 204
[21] H1 and ZEUS Collaborations 2015 *Eur. Phys. J. C* **75** 580
[22] ATLAS Collaboration 2017 *Preprint* ATLAS-CONF-2017-010
[23] ATLAS Collaboration 2017 *Preprint* ATLAS-CONF-2017-067
[24] Eskola K J, Paakkinen P, Paukkunen H and Salgado C A 2017 *Eur. Phys. J. C* **77** 163
[25] Kovarik K *et al.* 2016 *Phys. Rev. D* **93** 085037
[26] ATLAS Collaboration 2017 *Preprint* ATLAS-CONF-2017-072